Journal of Nondestructive Evaluation (2018) 37:83
https://doi.org/10.1007/s10921-018-0536-7

Acoustic Emission Generation Behavior in A7075-T651 and A6061-T6 Aluminum Alloys With and Without Cathodic Hydrogen Charging Under Cyclic Loading

Hideo Cho[1] · Naoki Shoji[1] · Hiroaki Ito[2]

Received: 23 June 2017 / Accepted: 15 October 2018

Abstract
Acoustic emission (AE) signals from non-charged and cathodic hydrogen charged A7075-T651 and A6061-T6 samples under tension–tension cyclic loading conditions at various stress intensity factor ranges were monitored. Although the AE event counts per cyclic load (AE count rates) were proportional to the crack growth rates in all kind of the sample, the rates were less than unity. Many cracked inclusions were observed on the crack surfaces and were identified as AE sources. Large inclusions in both Al alloys were prone to be fractured. The AE count rate in the A7075 sample was 10 times higher than that in A6061. However, no significant difference in the AE count rates and fatigue crack growth between the non-charged and charged samples were observed.

Keywords Acoustic emission · Fatigue · Aluminum alloys · Hydrogen embrittlement · Inclusion fracture

1 Introduction

Hydrogen energy sources such as fuel cells are expected to help reduce greenhouse gas emissions from automobiles. Although fuel cell vehicles have already been commercialized, their widespread adoption will require the development of a hydrogen gas station as an infrastructure. The stations must be equipped with tanks for containing high pressure hydrogen gas. One of candidate materials for the tank wall is a carbon fiber reinforced tank with A6061 Al alloy primarily comprising Al, Mg, and Si as a liner, because the Al alloy has low susceptibility to a hydrogen environment. However, the cyclic loading resulting from filling and supplying gas to vehicles may produce fatigue cracks in the Al alloy liner over a long term of service. Many studies on fatigue crack growth in Al alloys under various conditions have been conducted since the 1960s, and recently, the influence of hydrogen gas environment on fatigue crack growth has been specifically assessed to ensure safe tank operation [1, 2]. Therefore, for safe long-term tank operation, it is necessary to implement a continuous real-time monitoring for fatigue crack initiation and growth in service.

Acoustic emission (AE) technique in one of powerful methods for real-time evaluation of integrity loss of the large structures such as bridges, containers and so on, because AE wave is generated by rapid elastic energy release induced by micro crack initiation and growth in a material. AE technique is expected to reveal fracture process or mechanism of the structure in service. AE measurement for detecting fatigue crack growth in various Al alloys have been studied. H. Chang et al. [3] reported that the AE count rate was proportional to the crack growth rate and that the change of plastic zone at the crack tip was the source of AE. The AE count rate for T7075-T6 alloy in corrosive solution of 3.5% NaCl aqueous solution was found to be higher than that under air environment due to hydrogen embrittlement of the Al alloy. Yoshida et al. [4] reported that burst-type AE in A6061-T6 alloy under tensile loading was observed before the elastic limit was reached and attributed it to another source of AE which is micro-intergranular cracks beneath the fracture surface. Moreover, McBride et al. [5] reported AE sources in 7075 alloy under tensile loading, hypothesizing that the source may have been an inclusion fracture that occurred ahead of the crack tip in the proximity of the plastic zone boundary. Several possible AE sources have been reported

✉ Hideo Cho
cho@me.aoyama.ac.jp

[1] Aoyama Gakuin University, 5-10-1 Fuchinobe, Chuo-ku, Sagamihara, Kanagawa 252-5258, Japan

[2] Kindai University, 1 Takaya Umenobe, Higashi-Hiroshima, Hiroshima 739-2116, Japan

Published online: 24 October 2018

Table 1 Chemical compositions of A7075 and A6061 Al alloys

Material	Si	Fe	Cu	Mn	Mg	Cr	Zn	Ti	Al
A7075	0.08	0.19	1.7	0.02	2.4	0.19	5.5	0.02	Bal.
A6061	0.57	0.40	0.27	0.04	0.96	0.23	0.01	0.04	Bal.

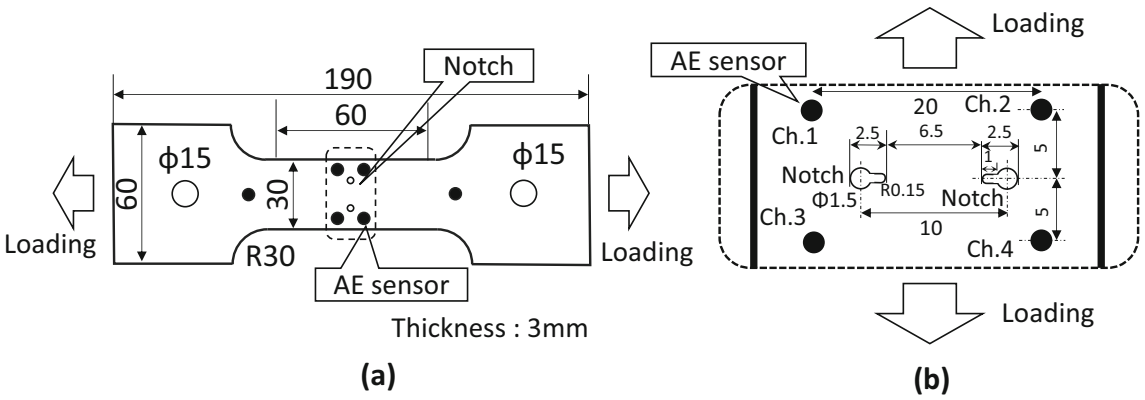

Fig. 1 Illustration of sample, notches and acoustic emission sensor location. **a** Sample shape. **b** Expanded area around notches

in Al alloys. For accessing the integrity of the containers for high pressure hydrogen gas, the physical meaning of AE source in the Al alloys which is directly exposed to hydrogen gas should be clear.

In this study, to clarify the sources of AE in two Al alloys—A7075-T651, which has high susceptibility to hydrogen and A6061-T6, which has low susceptibility—under cyclic loading conditions and characterize the influence of hydrogen on the AE count rate and fatigue crack growth rate, cathodic hydrogen charged and non-charged A7075-T651 and A6061-T6 alloy samples were submitted to fatigue testing at various stress intensity factor ranges ΔK while performing AE measurements.

2 Experimental Setup

A7075-T651 and A6061-T6 Al alloys were prepared for the samples. Table 1 showed chemical composition of both Al alloys. The both alloys with thicknesses of 3 mm were machined into tensile test specimens, as shown in Fig. 1a. The two 0.3-mm-wide and 1-mm-long notches shown in Fig. 1b were introduced at the center of each sample using a wire-discharged machine. The radius of curvature at the notch tip was ~ 0.15 mm. Hydrogen was catholically charged onto a 10 mm × 30 mm square-shaped region around the notches at a current density of 5 mA/cm^2 for 24 h in 0.2% boric acid + 0.24% KCl + 0.015% thiourea solution and then the sample was retained in air environment at room temperature for a couple of weeks to cause diffusible hydrogen to be emitted. As the cathodic hydrogen charging produced many pitting holes on the surface, those holes were removed out by polishing with abrasive papers of #320–#1500 prior to the fatigue test. The tension–tension cyclic loading test with a 20 Hz sinusoidal load was performed over various values of stress intensity factor range, ΔK. AE produced during fatigue crack growth was measured using four small AE sensors located at the corners of the 20 mm × 10 mm square area as shown in Fig. 1b. Resonance frequency of the AE sensor ranges from 200 to 450 kHz and its diameter is 4 mm. The side of fatigue crack from which AE was generated was determined by the arrival times of the AE signals. Two additional AE sensors were located near the loading pins with diameter of 15 mm to identify the noise from the friction between the pin and the sample. The output voltage of the AE sensors was amplified by 40 dB using pre-amplifiers and then fed to a computer via a 100–300 kHz band-pass filter. Sampling interval and points are 200 ns and 4096 points, respectively. AE was monitored during cyclic loading test. The load measurements were synchronized with AE detection, and crack lengths were measured by taking replicas of the respective cracks at the desired loading cycle. Each crack growth rate and stress intensity factor were calculated from the crack length, the load and the number of cycle.

3 AE Generation Behavior Under Cyclic Loading Test

3.1 Results for Non-charged A7075 and A6061 Al Alloy Samples

In the cyclic loading testing, the minimum value of K was maintained at 1 MPa m$^{1/2}$ and the maximum values of K were

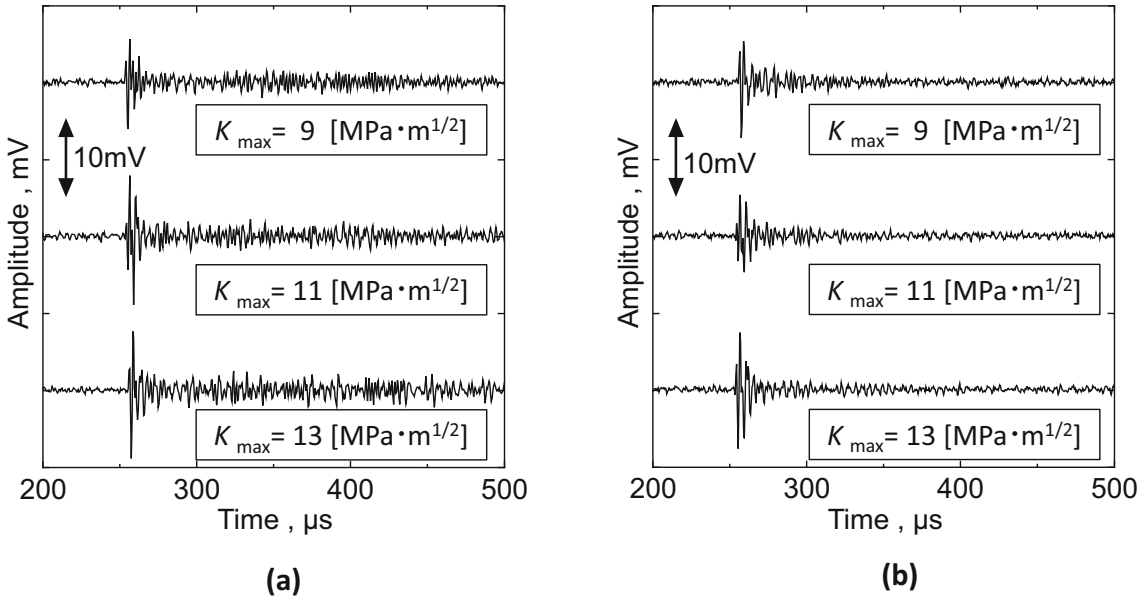

Fig. 2 Typical AE waveforms during cyclic loading for A7075 and A6061 samples without hydrogen charging at each K_{max}. **a** A7075-T651 sample. **b** A6061-T6 sample

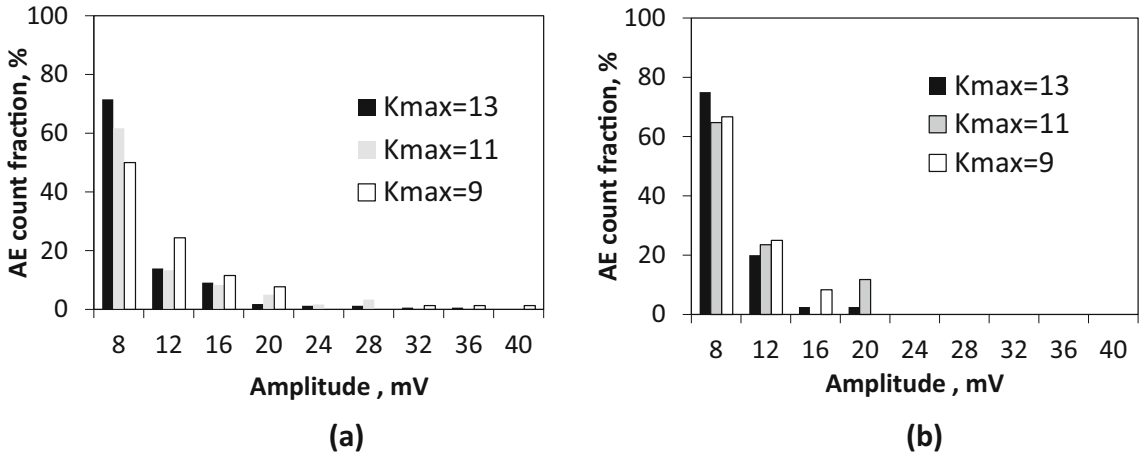

Fig. 3 Amplitude distributions of detected AE at load ratios grater than 0.9 for A7075 and A6061 samples without hydrogen charging. **a** A7075-T651 sample. **b** A6061-T6 sample

9, 11, and 13 MPa $m^{1/2}$ for avoiding fatigue crack surface contact or crack closer. Figure 2 shows typical AE signals taken by the four sensors surrounding the crack area for the non-charged A7075 and A6061 samples at the three K maxima. AE waves propagates as Lamb waves because the thickness of the sample is as thin as 3 mm. Most AE was of the burst type and was almost the same waveform, as shown in Fig. 2; this suggests that the AE source could be a brittle fracture with the same fracture mechanism in the samples. The load ratio at the AE detection timing, which is defined by the operational load divided by maximum load, was measured to be above 0.9 for most AE. This means AE sources may be accompanied with fatigue crack growth.

Figure 3 shows the AE amplitude distribution during crack growth at the three K maxima or ΔK. The AE amplitude distribution showed similar behavior in the both sample and is independent of the K maximum and the Al alloy. This suggested that crack volumes related to AE amplitude would be the same in the both samples and would not depend on both the size of plastic deformation zone and the crack growth per one cycle loading. Most AE showed the amplitude less than 12 mV. High amplitude AE signals above 24 mV suggesting large fracture volume were observed only in the A7075 sample. Figure 4 shows relation between the average crack growth rate and the AE count rate for both non-charged samples. The AE count rate was defined by the number of AE

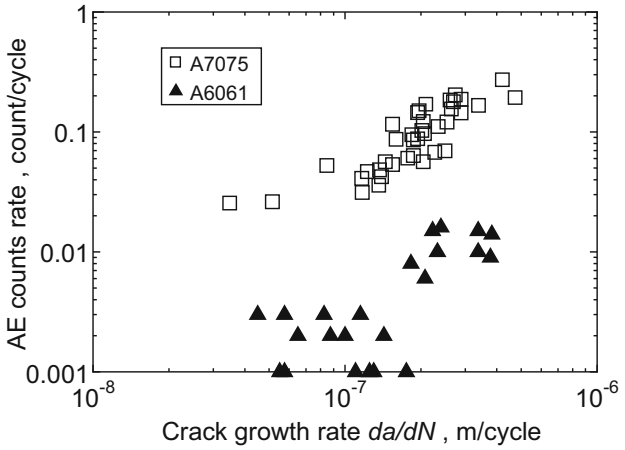

Fig. 4 AE count rates for A7075 and A6061 samples without hydrogen charging as a function of fatigue crack growth rate

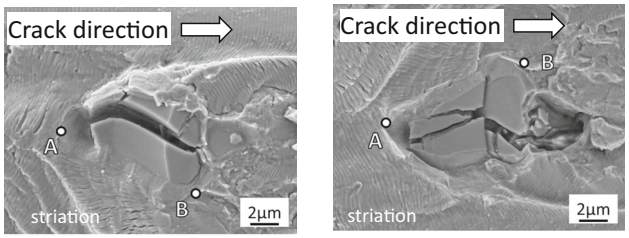

Fig. 6 SEM images of an identical cracked inclusion on both side of the crack surface for the A7075 sample without hydrogen charging. **a** Upper crack surface. **b** Lower crack surface

detections per one load cycle. The AE count rates in the both sample linearly increased with the crack growth rates following a log–log relation. This result is similar to that reported by Chang et al. [3] and would be useful for monitoring fatigue crack growth in Al alloy. The AE count rate for the non-charged A7075 sample was almost 10 times higher than that for the non-charged A6061 sample at the same crack growth rate. However, for both samples, the AE count rate was lower than unity per one load cycle especially in A6061 sample. It implies that the source of AE was neither a change in the plastic zone at the crack tip nor a striation formation mechanism which have been proposed by Change et al. [3]. No other micro-intergranular type cracks which was reported by Yoshida et al. [4] was observed.

In order to discuss the relation between AE generation and fatigue crack growth, we observed crack surfaces. Figure 5 shows scanning electron microscope (SEM) observation of cracked inclusions on a fatigue crack surface and energy dispersive spectroscopy (EDS) analysis results for A7075 and A6061 samples after the fatigue tests. In both samples, many cracks in the inclusions were observed on the fracture surfaces. Main AE source in the Al alloys would be the fracturing of these kind of inclusions which McBride et al. [5] also suggests in A7075 Al alloy. A striation pattern whose intervals mean crack growth rate, was also observed around the inclusion and the interval is much smaller than the inclusion size. This result supports the fact that AE did not generate per one cycle loading and AE count rate is much lower than unity. On the other hand, the amplitude of AE would depends on the size of the inclusions and did not relate with crack growth rate. EDS analysis further revealed that in both samples most of the cracked inclusions comprised Fe and Cu in the A7075 sample or Si and Mg in both samples. The number of Mg–Si inclusions were fewer than Fe–Cu inclusions in the A7075. An identical cracked inclusion on the upper and lower crack surfaces is shown in Fig. 6, where Points A and B in the two photos indicate the same location. The crack patterns are complicated and the patterns on the upper and lower crack surfaces differ, suggesting that these cracks initiated following a main fracture of the inclusion into two sections owing

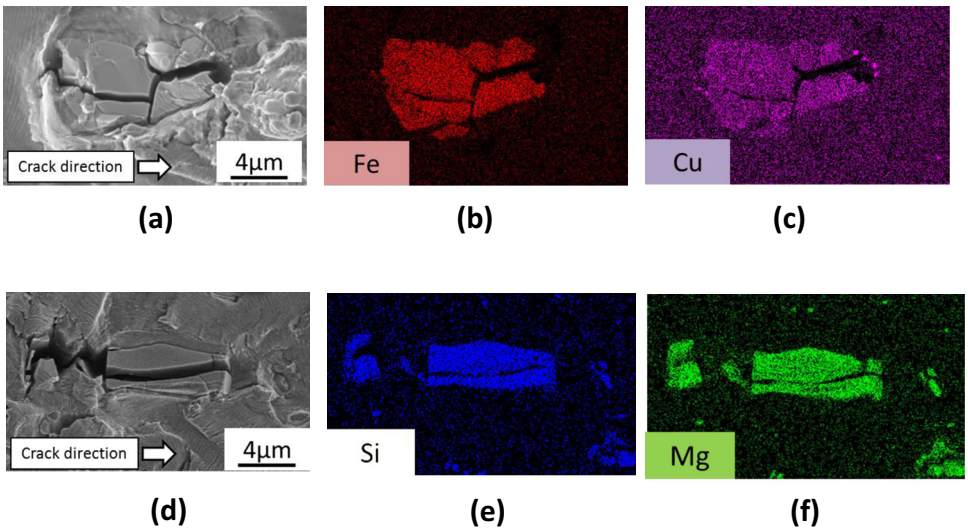

Fig. 5 SEM images of cracked inclusions in A7075 (upper) and A6061 (lower) on fatigue crack surface and EDS analysis of their inclusions. **a** SEM image(A7075). **b** Fe component. **c** Cu component. **d** SEM image(A6061). **e** Si component. **f** Mg component

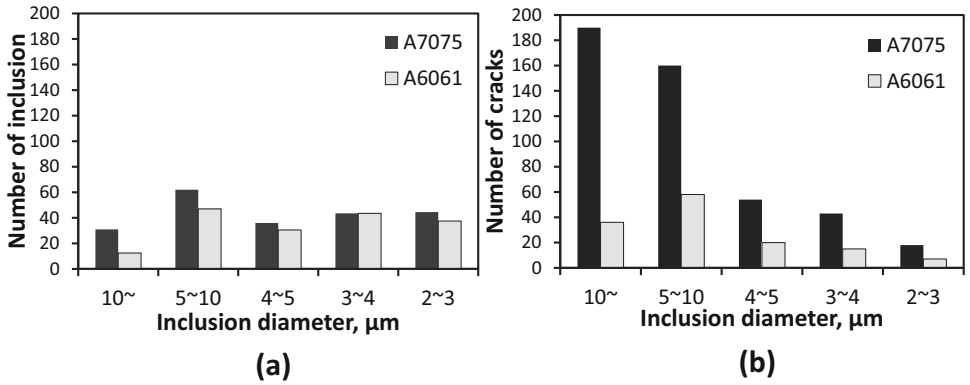

Fig. 7 Distributions of inclusion number and total number of cracks in one inclusion for A7075 and A6061 samples without hydrogen charging. **a** Number of inculsion. **b** Total number of cracks

to the tensile load in the plastic region ahead of the crack tip. This implied a couple of AE events would be initiated by one inclusion. Figure 7 shows the number of inclusion and the number cracks in the inclusions (b) for both samples at a K maximum of 11 MPa $m^{1/2}$. The observation area is equal to 0.024 mm^2. The size of inclusion was measured using the diameter of a circumscribed circle for each inclusion. The number of inclusions and their size distributions were similar for both samples, and the density of inclusion was $9.1 \times 10^4/mm^2$ and $7.1 \times 10^4/mm^2$ in the A7075 and A6061 samples, respectively. However, the number of cracks observed on the inclusions in the A7075 sample was much higher than that in the A6061 sample, especially in larger inclusions of above 5 μm; thus, the inclusions in the A7075 sample, which comprised Fe and Cu, were more brittle than the Si–Mg inclusions in the A6061 sample. The difference in the number of cracks corresponds to the AE count rate during cyclic load testing, as shown in Fig. 4. The AE count rate depends on both size and chemical composition of inclusions as well as the fatigue crack growth rate.

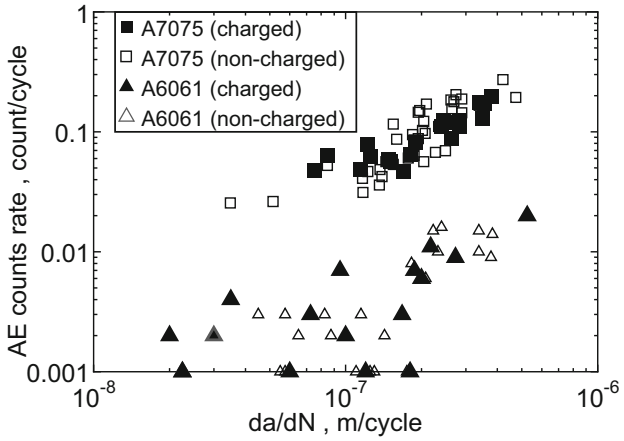

Fig. 8 AE count rates for A7075 and A6061 with hydrogen charging as a function of fatigue crack growth rate (closed symbols). AE count rate for the samples without hydrogen charging were shown as open symbols

3.2 Results for Cathodic Hydrogen Charged A7075 and A6061 Al Samples

Hydrogen environment affects mechanical properties such as proof stress, elongation in Al alloy and also leads hydrogen embrittlement and stress corrosion cracking [6]. Also fatigue life in some Al alloys lowers due to hydrogen immigration into the alloys [7]. Therefore in this section, the effect of hydrogen on the relation between AE generation rate and crack growth rate will be discussed by use of cathodic hydrogen charging to the samples prior to the cyclic tests.

Figure 8 shows AE count rate as a function of crack growth rate for both charged samples. The AE count rate for the non-charged sample is also plotted as open symbols. No difference in terms of AE count rate between the non-charged and charged samples is observed, nor is there any significant change in the relation between crack growth rate and ΔK. As was true for the non-charged samples, many cracked inclusions are seen on the fatigue crack surfaces. The AE source in the charged sample was also fracturing of the inclusions and this mean that the inclusion did not show hydrogen embrittlement. Although A7075 Al alloy is susceptible to a hydrogen environment, there is little difference between the charged and non-charged samples surfaces in terms of crack growth rate, AE count rate, or number of inclusion fractures. To further study the influence of hydrogen on both Al alloys, a tensile test was also performed on both non-charged and charged samples with AE measurement. Figure 9 shows stress–strain curves for the A7075(a) and A6061(b) Al alloy samples with and without hydrogen charging. A tensile test was performed at a crosshead speed of 2.0×10^{-2} mm/s for all samples. In both Al alloys, proof stress of 0.2%, Young's modulus, and strength showed nearly the same results. Only the fracture strain in the charged A7075 sample was lower than that in the non-charged sample and the fracture strain in charged and non-charged A6061 showed almost identical; Osaki et al. reported the same results [8]. The number of AE count in A7075 samples were much larger than that

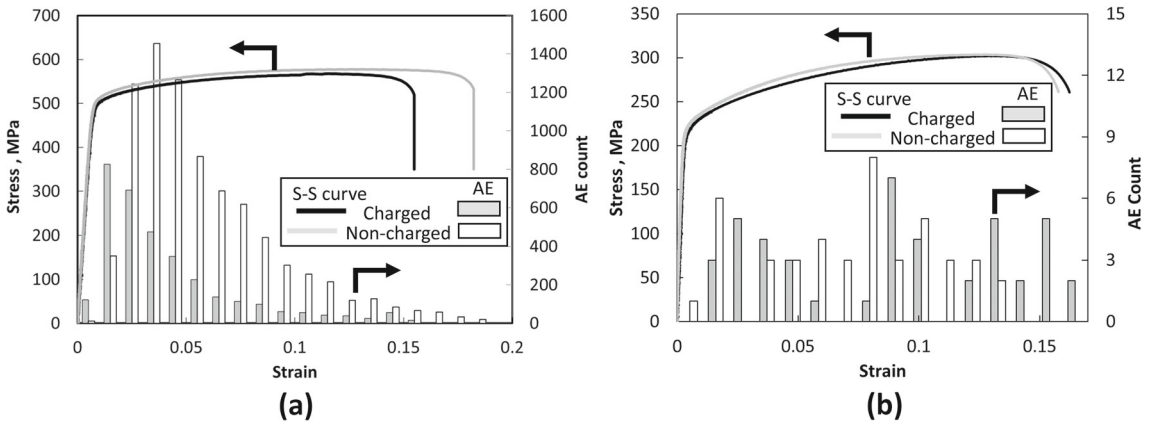

Fig. 9 Strain-stress curves for A7075 and A6061 with and without hydrogen charging with AE count. **a** A7075. **b** A6061

in A6061 samples. SEM observation of the sample surfaces after testing revealed that the sources of AE were inclusion fractures as well as in the cyclic loading test. This low AE count in A6061 alloy samples is caused by the same reason in cyclic loading test due to inclusion size. Previous researchers have also reported that inclusion fractures occurred in A7075 and A 6061 alloys during tensile loading tests [9, 10]. In this study, the onset strain of AE generation in the charged A7075 sample was lower than that in the non-charged sample suggesting inclusion fracture in the charged sample started at low strain region compared to the non-charged sample. This would be caused by the higher stress applied to the inclusion in the low strain region. The presence of hydrogen led to local plastic deformation in high stress regions such as that ahead of a crack tip or the interface between an inclusion and an Al alloy matrix [11]. However, while fatigue crack growing, the influences of hydrogen on both fatigue crack growth and AE count rate even in A7075 alloy sample have not been observed. This mean that inclusion fracture in the plastic region ahead of the crack tip would not affected fatigue crack growth.

4 Conclusions

In order to discuss the feasibility of acoustic emission technique to monitoring integrity of the container for high pressure hydrogen gas, the AE sources in two different Al alloys A7075-T651 which have high susceptibility to hydrogen and A6061-T6 which are immune to hydrogen and is used for the container as a metallic liner, under cyclic and static loading condition were studied. The influence of hydrogen on AE generation behavior was also studies. The results obtained in this study are as follows:

1) The AE count per cyclic loading increased with the crack growth rate and was < 1 for a crack growth rate of $< 10^{-6}$ m/cycle for both A7075 and A6061. Many cracked inclusions comprising Fe–Cu and Mg–Si systems were observed on crack surfaces in both samples. AE sources may be inclusion fractures. The AE count rate in A7075 was 10 times higher than that in A6061. Although the inclusion densities in A7075 and A6061 were nearly identical, many larger inclusions in A7075 were observed than in A6061. Complicated crack pattern on the inclusion was observed and the patterns on the corresponding inclusions on the upper and lower fatigue crack surfaces differ. The difference in terms of the number of cracks corresponds to the AE count rate.
2) The relation between the AE count rate and crack growth rate in the charged A7075 and A6061 samples was nearly the same as it was between the corresponding non-charged samples. Many cracked inclusions were also observed in both charged and non-charged samples. Tensile testing showed that the influence of hydrogen was limited to fracture elongation and onset of AE generation timing on the A7075 sample, with no significant difference measured as a result of 0.2% proof stress, ultimate strength and AE generation behaviors on both alloys.

References

1. T. Ogawa, S. Hasunuma, N. Sogawa, T. Yoshida, T. Kanezaki and S. Mano, (2014), "Characteristics of fatigue crack growth and stress corrosion cracking in aggressive environments of aluminium alloys for hydrogen gas containers.", ASME 2014 pressure vessels and piping conference, paper No. PVP2014-28236
2. Tomioka, J., Kiguchi, K., Tamura, Y., Mitsuishi, H.: Influence of temperature on the fatigue strength of compressed-hydrogen tanks for vehicles. Int. J. Hydrog. Energy **36**(3), 2513–2519 (2011)
3. Chang, H., Han, E., Wang, J.Q., Ke, W.: Acoustic emission study of corrosion fatigue crack propagation mechanism for LY12CZ and 7075T-6 aluminium alloys. J. Mater. Sci. **40**, 5669–5674 (2005)
4. K. Yoshida, T. Tokuyama, Y. Yashuhara and H. Nishino, (2012), Evaluating of AE sources during tensile deformation of Al–Mg–Si alloys with different heat treatment. In: Proceedings of 30th Euro-

pean conference on acoustic emission testing and 7th international conference on acoustic emission
5. McBride, S.L., MacLachlan, J.W., Paradis, B.P.: Acoustic emission and inclusion fracture in 7075 aluminium alloys. J. Nondestruct Eval **2**(1), 35–41 (1981)
6. Ambat, R., Dwarakadasa, E.S.: Effect of hydrogen in aluminum and aluminum alloys: a review. Bull. Mater. Sci. **10**(1), 104–114 (1996)
7. Deya, S., Chattoraja, I., Sivaprasada, S.: Effect of hydrogen on mechanical degradation and fatigue in 7075 aluminium alloy with in situ hydrogenation. Proc. Eng. **114**, 461–469 (2015)
8. Osaki, S., Ikeda, J., Kinoshita, K., Sasaki, Y.: Hydrogen embrittlement properties of 7075 and 6061 aluminum alloys in humid air. J. Jpn. Inst. Light Met. **56**(12), 721–727 (2006). **(In Japanese)**
9. Blasundaram, A., Gokhale, A.M., Graham, S., Horstemeyer, M.F.: Three-dimensional particle cracking damage development in an Al-Mg-base wrought alloy. Mater. Sci. Eng. A **335**, 368–383 (2003)
10. Lugo, M., Jordan, J.B., Horstemeyer, M.F., Tschopp, M.A., Harris, J., Gokhale, A.M.: Quantification of damage evolution in a 7075 aluminium alloy using an acoustic emission. Mater. Sci. Eng. A **528**, 6708–6714 (2011)
11. Gang, L., Qing, Z., Nicholas, K., Efthimios, K.: Hydrogen-enhanced local plasticity in aluminium: An Ab Initio study. Phys. Rev. Lett. **87**(9), 095501 (2001)